



Using free air CO₂ enrichment data to constrain land surface model projections of the terrestrial carbon cycle

Nina Raoult^{1*}, Louis-Axel Edouard-Rambaut², Nicolas Vuichard¹, Vladislav Bastrikov³, Anne Sofie Lansø⁴, Bertrand Guenet⁵, and Philippe Peylin¹

¹Laboratoire des Sciences du Climat et de l'Environnement, LSCE/IPSL, CEA-CNRS-UVSQ, Université Paris-Saclay, 91191, Gif-sur-Yvette, France

²CIRAD, UMR SELMET, Station de Ligne-Paradis – 7 chemin de l'IRAT – 97410 Saint-Pierre – Réunion, France

³Science Partners, Paris, France

⁴Department of Environmental Science, Aarhus University, Aarhus, Denmark

⁵Department of Geosciences Ecole normale supérieure (ENS), 24 Rue Lhomond, 75231 Paris Cedex 05, France

*now University of Exeter, United Kingdom

Correspondence: Nina Raoult (n.m.raoult2@exeter.ac.uk)

Abstract. Predicting the responses of terrestrial ecosystem carbon to future global change strongly relies on our ability to model accurately the underlying processes at a global scale. However, terrestrial biosphere models representing the carbon and nitrogen cycles and their interactions remain subject to large uncertainties, partly because of unknown or poorly constrained parameters. Data assimilation is a powerful tool that can be used to optimise these parameters by confronting the model with observations. In this paper, we identify sensitive model parameters from a recent version of the ORCHIDEE land surface model that includes the nitrogen cycle. These sensitive parameters include ones involved in parameterisations controlling the impact of the nitrogen cycle on the carbon cycle and, in particular, the limitation of photosynthesis due to leaf nitrogen availability. We optimise these ORCHIDEE parameters against carbon flux data collected on sites from the Fluxnet network. However, optimising against present-day observations does not automatically give us confidence in the future projections of the model, given that environmental conditions are likely to shift compared to present-day. Manipulation experiments give us a unique look into how the ecosystem may respond to future environmental changes. One such experiment, the Free Air CO₂ Enrichment experiment, provides a unique opportunity to assess vegetation response to increasing CO₂ by providing data at ambient and elevated CO₂ conditions. Therefore, to better capture the ecosystem response to increased CO₂, we add the data from two FACE sites to our optimisations, in addition to the Fluxnet data. We use data from both CO₂ conditions of the Free Air CO₂ Enrichment experiment, which allows us to gain extra confidence in the model simulations using this set of parameters. We find that we are able to improve the magnitude of modelled productivity. Although we are unable to correct the interannual variability fully, we start to simulate possible progressive nitrogen limitation at one of the sites. Using an idealised simulation experiment based on increasing atmospheric CO₂ by 1% per year over 100 years, we find that the rate of CO₂ fertilisation is much lower when Free Air CO₂ Enrichment data has been in the optimisation.



20 1 Introduction

Since the start of the industrial era, the atmospheric CO₂ concentration has risen from around 278 ppm in 1850 to 417.2 ppm in 2022 (Friedlingstein et al., 2022). Increases in atmospheric CO₂ lead to increases in leaf-scale photosynthesis and intrinsic water-use efficiency, which in turn have the potential to increase plant growth, vegetation biomass, and soil organic matter (Walker et al., 2021). Known as CO₂ sequestration, this process transfers carbon from the atmosphere into terrestrial ecosystems. Indeed, terrestrial ecosystems currently remove about 30% of the CO₂ emitted by human activities each year (Friedlingstein et al., 2020). However, predicting how this carbon sink will evolve under increasing atmospheric CO₂ remains a challenge, especially due to the large uncertainties in the magnitude of carbon-climate feedbacks. Furthermore, the terrestrial ecosystem's ability to store carbon will be influenced by other processes, for example, nutrient limitations (Zaehle and Dalmonch, 2011) - most notably nitrogen, which is a key component controlling the carboxylation activity of the RubisCo in the photosynthetic tissue of the plant.

The large uncertainties in terrestrial carbon projections are largely related to the uncertainty in land surface models, including parametric uncertainty, which relates to the parameter values used in each parameterisation (Zaehle et al., 2005). The first land surface models were developed to provide a physical boundary to meteorology processes. As these models progressed, terrestrial biogeochemical cycles were implemented, simulating leaf gas exchange through Ball-Berry stomatal conductance and plant productivity based on Farquhar photosynthesis (Bonan, 2015). More recently, land surface models have moved from a big leaf model to multi-canopy schemes (Naudts et al., 2015), and started to include the nitrogen cycle and its constraints on the terrestrial carbon balance (e.g., LPJ: Prentice (2008), OCN: Zaehle and Friend (2010), ORCHIDEE-CN: Vuichard et al. (2019), CLM: Fisher et al. (2019)). However, with each new process and complexity added to the model, we add more internal model parameters, which in turn can add more uncertainty. Even though these parameters are generally chosen to represent measurable real-world quantities (e.g., leaf area, plant root depth), their default values are often issued from specific experiments studying the processes at different scales to those used in land surface models. Therefore it is important to confront simulated model outputs against independent data.

There are a lot of data with which we can evaluate model simulations from vast in situ networks (e.g., Fluxnet, Pastorello et al. (2020)) to state-of-the-art satellite retrievals (e.g., sentinel missions, Malenovský et al. (2012)). It is important to evaluate land surface models against these types of data since they help increase confidence in the model simulations. Furthermore, these data can also be used to optimise models through data assimilation. Data assimilation methods can be used to perform parameter optimisation where uncertain parameters are tuned to minimise the difference between simulated model output and observed quantities. Fluxnet eddy-covariance data has already been used to optimise model parameters in most land surface models; e.g., ORCHIDEE (Kuppel et al., 2012), BETHY (Knorr and Kattge, 2005), JULES (Raoult et al., 2016), Noah (Chaney et al., 2016) and CLM (Post et al., 2017). However, evaluating and optimising against historical trends and present-day observations does not necessarily give us confidence in the future projections of the model, given that future environmental conditions are likely to shift compared to present-day (Wieder et al., 2019).



Fortunately, manipulation experiments give us a unique look into how the ecosystem may respond to future environmental change. One such experiment, the Free Air CO₂ Enrichment experiment (FACE; Norby et al. (2010); Walker et al. (2018)), provides a unique opportunity to assess vegetation response to increasing CO₂. FACE experiments are conducted across several vegetation types and typically consist of two plots: one where CO₂ is fumigated to high concentrations and one left as a control. Many studies have used these experimental sites to anticipate the future of terrestrial ecosystems. In 2005, Ainsworth and Long (2005) summarised results from 120 peer-reviewed articles describing physiology and production in the 12 large-scale FACE experiments (475–600 ppm). More recently, Ainsworth and Long (2021) discussed how the last 30 years of FACE experiments improved our understanding of crop productivity under future elevated atmospheric CO₂.

In particular, two decade-long FACE experiments in temperate forests of the southeastern U.S. (Duke and Oak Ridge National Laboratory (ORNL)) have been predominately studied to test the representations of carbon–nitrogen cycle processes in land surface models. A full intercomparison of 11 land surface models (Medlyn et al., 2015) demonstrated how these data could be used to evaluate models looking at the effect of ambient and elevated CO₂ on water (De Kauwe et al., 2013), carbon (De Kauwe et al., 2014) and nitrogen (Walker et al., 2014; Zaehle et al., 2014). These two sites were further used in Wieder et al. (2019), where they showed how these experimental manipulations could be incorporated into the model benchmarking tools to help increase confidence in terrestrial carbon cycle projections. FACE experiments can also be used to identify processes that are not well caught by land surface models. For instance, Walker et al. (2019) showed that elevated CO₂ changed carbon allocation to the wood, and none of the models tested were able to reproduce this observation. Combined with warming experiments within a factorial design, the FACE experiments can also be very useful to evaluate how much the model are able to reproduce the single effect of elevated CO₂ versus the effect of elevated CO₂ when other drivers are changing (De Kauwe et al., 2017). More recently, Sulman et al. (2019) used these two sites to test the effect of adding symbiotic nutrient acquisition strategies to land surface models and Caldararu et al. (2020) to assess a whole-plant growth optimality approach in improving the representation of leaf nitrogen content compared to existing empirical approaches. The two sites are also the sites we will focus on in this study.

We use these sites to check whether the parameterisations and parameters used in a land surface model are able to capture the ecosystem response to increased CO₂. Furthermore, by optimising a land surface model to both ambient and elevated conditions, we will gain extra confidence in the model projections using this set of parameters. Our study will be the first, to our knowledge, to do this with a global land surface model.

Using the ORCHIDEE land-surface model as an example, in this paper, we will show the potential of using manipulation sites to not only optimise unknown model parameters but also increase confidence in the optimised model projections by reducing parameter uncertainty. Furthermore, by optimising parameters linked primarily to the nitrogen cycle, as well as considering nitrogen-limited FACE sites, we will get an insight into the nitrogen-limiting effect on the fertilising effect of CO₂. This study also looks at how FACE data can complement Fluxnet data in a general optimisation procedure. As such, we aim to answer the following questions:

- Using data assimilation, can we improve the representation of the simulated productivity of the new nitrogen-version of ORCHIDEE over Fluxnet and FACE sites (under both ambient and elevated conditions)?



- What is the benefit of adding FACE data on top of Fluxnet data when optimising a land surface model?
- How does the future evolution of terrestrial productivity change when simulated using different sets of optimised parameter values?
- Can these experiments help us to describe better the future fertilising effect of CO₂ under possible nitrogen limitation?

2 Methods

2.1 Model

2.1.1 The ORCHIDEE land surface model

95 The ORCHIDEE (ORgainizing Carbon and Hydrology in Dynamic Ecosystems) model is a global terrestrial ecosystem model developed at IPSL (Institut Pierre Simon Laplace, France). It simulated the energy (Ducoudré et al., 1993), water (de Rosnay and Polcher, 1998), carbon (Krinner et al., 2005), and nitrogen (Zaehle and Friend, 2010; Vuichard et al., 2019) exchanges between the land surface and the atmosphere. This model can be run at various spatial resolutions, ranging from site to global simulations, and over different timescales from one day to thousands of years. ORCHIDEE can be run as a stand-alone model
100 driven by meteorological forcing or as part of the IPSL Earth System Model (Boucher et al., 2020; Lurton et al., 2020).

In ORCHIDEE, the different types of vegetation are discretised in Functional types (PFTs, Plant Functional Types) defined by plant metabolism, phenology, type of leaves and local climate. There are a total of 15 PFTs in ORCHIDEE; eight for the forests, four for the grasslands, two for the crops and one for bare soil. The model describes the different stocks of biomass in the whole soil-plant continuum. There are nine stocks of biomass in the plant; the leaf, the above and below-ground sapwood,
105 the above and below-ground heartwood, the fruits, the roots, and the long-term and short-term (available to use) reserves. For litter, there are six carbon stocks; metabolic, structural and woody above- and below-ground. Finally, there are four stocks for the soil organic matter; surface, active, slow and passive.

The litter pools are limited by the fall and death of tissues. The pools of organic matter in the soils are alimented by the decomposition of the organic matter in the different pools of the litter. The decomposition of the organic matter is characterised
110 by a fixed residence time for each litter and/or soil pool modulated by environmental conditions.

The carbon/nitrogen ratio of leaf biomass is variable, controlled by a supply/demand scheme while the C/N ratio of the other plant pools is a fixed proportion of the leaf C/N ratio. A specific C/N ratio is set for each soil pool, which varies as a function of the mineral nitrogen in soils. There are also additional mineral nitrogen pools in soils for ammonium, nitrate, nitrous oxides, nitrogen oxides and dinitrogen. The inputs of nitrogen in the soil/plant system are considered deposition, fertiliser and manure
115 inputs and biological fixation. Nitrogen losses are associated with leaching, lixiviation and emissions of ammonia, nitrous oxide, nitrogen oxides and dinitrogen.

The nitrogen component for ORCHIDEE was first developed and evaluated inside OCN, a version of the ORCHIDEE model (Zaehle and Friend (2010)). However, at the time, it was not embedded into the operational ORCHIDEE version used



120 in coupled experiments. This component has been recently updated and is now included in default ORCHIDEE runs (Vuichard et al., 2019). This has notably permitted studies of the interactions between the carbon and nitrogen cycles and their effect on gross primary production (GPP). The version of ORCHIDEE used in our study (ORCHIDEEv3, r6863) is more recent than the one used Vuichard et al. (2019). It has been used in the multi-model ensemble for the Global Carbon Budget 2020 (Friedlingstein et al., 2022) but has not yet been optimised against independent data. As such, the initial fit of the model to the Fluxnet data is different than that shown in Vuichard et al. (2019).

125 2.1.2 Model parameters

An initial list of parameters was compiled based on parameters used in past ORCHIDEE optimisations. This was extended to include parameters of the new nitrogen module selected using the expert knowledge of the module developers. Using a Morris sensitivity analysis (Morris, 1991), we removed all parameters showing no sensitivity to the different modelled outputs tested (i.e., net primary product (NPP) and leaf-area index (LAI)). All remaining parameters were optimised in this study (Table 1).
130 These parameters represent key parameters of the model controlling photosynthesis, carbon and nitrogen allocation, respiration and global nitrogen cycle behaviour. In addition, the KSoil parameter was used to control the initial carbon and nitrogen stocks. This parameter makes up for the fact that we cannot reconstruct each site's land-use history and its impacts on the present-day soil carbon stocks. Instead, we add the KSoil parameter in the optimisation, a multiplication factor applied on some soil carbon and nitrogen pools (slow, passive and labile) to change their initial values. A similar parameter has been used in many previous
135 ORCHIDEE optimisation studies to control the initial carbon stocks of the model (e.g., Santaren et al., 2007; Kuppel et al., 2012; Bastrikov et al., 2018).

For each PFT, the Morris score for each parameter has been normalised by the most sensitive parameter. The normalised Morris sensitivity scores are shown in Table 1 and help us understand which are the most sensitive parameters. We see that for sites with a strong seasonal cycle, i.e., TeBS sites, the specific leaf area (SLA) phenology parameters are most sensitive. For
140 the evergreen sites, two of the nitrogen parameters NUE_{opt} and $K_{LAtSA, max}$ gain importance ranking as highly as SLA.

2.2 Data assimilation framework

The optimisations performed in this study relies on a Bayesian framework to include prior knowledge on the parameters (\mathbf{x}_b). Assuming that the errors associated with data observation, model output and parameters follow Gaussian distributions (Santaren et al., 2014), we seek to obtain a posterior optimal parameter set \mathbf{x}_{opt} which corresponds to the minimum of the cost
145 function $J(\mathbf{x})$:

$$J(\mathbf{x}) = (M(\mathbf{x}) - \mathbf{y})^T \mathbf{R}^{-1} (M(\mathbf{x}) - \mathbf{y}) + (\mathbf{x} - \mathbf{x}_b)^T \mathbf{B}^{-1} (\mathbf{x} - \mathbf{x}_b). \quad (1)$$

For a given parameter set \mathbf{x} , $J(\mathbf{x})$ measures the mismatch between observations \mathbf{y} and the corresponding model outputs $M(\mathbf{x})$, and the mismatch between the prior, or background, parameter set \mathbf{x}_b and \mathbf{x} . Each of these terms are weighted by their error covariances matrices, \mathbf{R} and \mathbf{B} for the observations and parameters respectively (Tarantola, 2005). Note that \mathbf{R} includes both
150 measurement and model errors.



Table 1. List of parameters used for the optimization with descriptions, default (prior) model values, ranges of variation, and normalised Morris scores denoting the relevant importance of each parameter (labelled "rk" for rank) - darker squares means more sensitive.

Parameter	Description	Temperate Broadleaf Summergreen (TeBS)				Temperate Needleleaf Evergreen (TeNE)			
		min	prior	max	rk	min	prior	max	rk
Nitrogen-related processes									
CTE _{bact}	Denitrification activity of bacteria	1e-04	5e-04	1e-03		1e-04	5e-04	1e-03	
CN _{leaf, max}	Maximum C/N ratio of the leaves	36	45	54		60	75	90	
CN _{leaf, min}	Minimum C/N ratio of the leaves	11	16	22		18	28	38	
k _N	Extinction ratio of N through the canopy	0.13	0.15	0.18		0.13	0.15	0.18	
FCN _{root}	N/C ratio of the roots/wood used to calculate allocation	0.6	1.0	1.2		0.6	1.0	1.2	
FCN _{wood}	relative to the leaf N/C ratio	0.06	0.087	0.12		0.06	0.087	0.12	
NUE _{opt}	Nitrogen use efficiency of Vcmax	23	33	43		10	20	30	
R _{leaf}	Fraction of N leaf/root that is recycled when leaves are	0.4	0.5	0.6		0.4	0.5	0.6	
R _{root}	senescent	0.1	0.2	0.3		0.1	0.2	0.3	
z	Root profile	0.2	0.8	3		0.25	1.0	4.0	
VMAX1 _{UPTAKE}	Maximal Uptake capacity of roots for ammonium	2	3	4		2	3	4	
VMAX2 _{UPTAKE}	Maximal Uptake capacity of roots for nitrates	2	3	4		2	3	4	
Allocation									
K _{LtoSA, max}	Maximum leaf to sapwood area ratio	9000	3750	9900		5768	3000	7500	
K _{LtoSA, min}	Minimum leaf to sapwood area ratio	300	2400	5500		150	800	5000	
K _{root}	Fine root specific conductivity	3e-07	4e-07	5e-07		3e-07	4e-07	5e-07	
K _{sap}	Maximal sapwood specific conductivity	2e-04	3e-04	4e-04		6e-04	8e-04	1e-03	
Phenology									
SLA	Specific leaf area at the time of the leaf productions	0.026	0.013	0.05		0.009	0.004	0.02	
SLA _{init}	Initial Specific leaf area at the bottom of the canopy	0.03	0.02	0.04		0.044	0.034	0.054	
L _{agecrit}	Critical Leaf Age	90	180	240		610	910	1210	
L _{fall}	Leaf Fall	8	10	12		N/A	N/A	N/A	
T _{senes}	Critical temperature for senescence	10	12	22		N/A	N/A	N/A	
Photosynthesis (carbon assimilation)									
k	Extinction ratio of the light through the canopy	0.3	0.5	1.0		0.3	0.5	1.0	
A ₁	Empirical factors involved in the calculation of fvpd	0.7	0.85	0.9		0.7	0.85	0.9	
B ₁		0.1	0.14	0.18		0.1	0.14	0.18	
Respiration									
FRAC _{growthresp}	Fraction of the GPP that is lost to growth respiration	0.2	0.28	0.36		0.2	0.28	0.36	
Q ₁₀	Parameter determining the temperature dependency of the heterotrophic respiration	0.0	0.69	1.1		0.0	0.69	1.1	
Spinup parameters (site dependent)									
KSoil	Multiplicative factor for initial soil carbon & nitrogen stocks	0.5	1	2		0.5	1	2	



There exist many different approaches we can use to find the set of parameters which minimizes $J(x)$. These range from simple manual tuning, which are very computationally demanding and inefficient, to more complex algorithms either based on deterministic gradient descent methods or stochastic random search methods. Using “ORCHIDAS”, the ORCHIDEE data assimilation tool developed at the Laboratoire des Sciences du Climat et de l’Environnement (Bastrikov et al. (2018)), we performed a couple of preliminary experiments to determine which algorithm to use. We tested a gradient descent method based on the L-BFGS-B algorithm (limited memory Broyden–Fletcher–Goldfarb–Shanno algorithm with bound constraints BFGS; Byrd et al. (1995)) and a random search method based on the genetic algorithm (GA; Goldberg and Holland (1988); Haupt and Haupt (2004)). We found that the GA method outperformed the gradient method in reducing the cost function. These initial results are coherent with Bastrikov et al. (2018)’s study, which optimised the gross primary productivity (GPP) and latent heat fluxes of a former version of ORCHIDEE against a number Fluxnet site measurements and also found that the GA algorithm outperformed the other methods, notably by allowing a full exploration of all parameter space.

The genetic algorithm consists in applying the laws of evolution to our set of parameters by considering the set of parameters as a chromosome, with each parameter as a gene. At each iteration, the algorithm fills k chromosomes with parameter values. The first pool of chromosomes is created by randomly perturbing the value of the parameter. For the following iterations, the chromosomes are created from the previous iterations’ chromosomes. Two processes come into play; a) a crossover process, where we have an exchange of genes between two chromosomes, and b) a mutation process, where random genes are perturbed. To ensure that the best chromosomes get the most descendants, each chromosome of each iteration gets ranked in function of the cost associated with the parameter’s value in the chromosome.

2.3 In situ data

In this study, we considered two sites from the FACE network in nitrogen-limited temperate forest ecosystems; Oak-Ridge (ORNL; Norby et al., 2010) - a site dominated by broad-leaf deciduous forests (TeBS, for Temperate Broadleaf Summergreen Forests) and Duke (DUKE; McCarthy et al., 2010) - a site dominated by needle-leaf evergreen forests (TeNE, for Temperate Needleleaf Evergreen Forests). For each site, we used the data from two experimental plots; one with unaffected atmospheric CO_2 , i.e. ambient (AMB), and one with elevated atmospheric CO_2 (ELE). Data are provided with error bars.

The version of ORCHIDEE used in this study has yet to be optimised against Fluxnet data using a Bayesian framework, as it was done with previous nitrogen-free versions of the model (e.g., Kuppel et al., 2012; Peylin et al., 2016). Therefore, we also considered TeBS and TeNE sites from the FLUXNET2015 dataset (Pastorello et al., 2020). This dataset provides gap-filled half-hourly meteorological data measured at each site (air temperature, humidity, pressure, wind speed, rainfall and snowfall rates, shortwave and longwave incoming radiation; see Vuichard and Papale (2015)). It also provides net carbon flux measurements, as such net ecosystems exchange (NEE) further split into gross primary production (GPP) and total ecosystem respiration (TER) following a classical night-time vs day-time flux partition Lasslop et al. (2010). For each of the two vegetation types, sites with over 60% vegetation coverage were kept. We excluded sites with too large discrepancies with the prior model output, such as with no apparent seasonal cycle, large data gaps, or with only one year of data. The list of in situ sites used can be seen in Table 2 partitioned by vegetation type.



Table 2. List of in situ FACE and Fluxnet sites used in the study. The Fluxnet sites are labelled by a country code (first two letters) and site name (last three letters). The FACE sites are both found in the US. The period corresponds to the available years of data for each of the sites.

Temperate Broadleaf Summergreen (TeBS)			Temperate Needleleaf Evergreen (TeNE)		
Site id	Years	Coordinates	Site id	Years	Coordinates
Free Air CO₂ Enrichment experiment sites					
ORNL	1999-2008	35.54, -84.20	DUKE	1996-2007	35.58, 70.5
FLUXNET2015 sites					
DE-Hai	2000-2012	51.08, 10.4	CZ-Bk1	2004-2008	49.50, 18.54
DK-Sor	1996-2014	55.49, 11.64	DE-Tha	1996-2014	50.96, 13.57
FR-Fon	2005-2014	48.48, 2.78	FR-LBr	1996-2008	44.72, -0.77
IT-Col	1996-2014	41.85, 13.59	IT-Lav	2003-2014	45.96, 11.28
IT-PT1	2002-2004	45.20, 9.06	IT-Ren	1998-2013	46.57, 11.43
IT-Ro1	2000-2008	42.41, 11.93	IT-SRo	1999-2012	43.73, 10.28
IT-Ro2	2002-2012	42.39, 11.92	NL-Loo	1996-2013	52.17, 5.74
US-Ha1	1991-2012	42.54, -72.17	RU-Fyo	1998-2014	56.46, 32.92
US-MMS	1999-2014	39.32, -86.41	US-Blo	1997-2007	38.90, -120.63
US-UMB	2000-2014	45.56, -84.71	US-GLE	2004-2014	41.37, -106.24
US-WCr	1999-2014	45.81, -90.08	US-Wi4	2002-2005	46.74, -91.17

185 2.4 Performed experiments

Before performing the optimisations, for each of the sites in this study, a two-step spin-up was performed. The first step helped to put the prognostic variables, including vegetation state, soil carbon pools, and soil moisture content at equilibrium. The available meteorological forcing was cycled over several millennia (with pre-industrial CO₂ concentrations) to ensure that the long-term net carbon flux was close to zero. After reaching the equilibrium, a second simulation was performed (transient) from the year 1860 to one year before the first forcing year while increasing CO₂ concentration at each simulation year following global historical observations.

Once spun up, we performed two main sets of optimisations. The first is over the Fluxnet sites only while the second also includes data from the FACE sites. Due to the CO₂ fumigation over FACE sites, NEE is not measured at these sites, and therefore, GPP and TER estimates cannot be derived. Instead, for the FACE sites, we have annual net primary production (NPP) and daily leaf area index (LAI) data. Throughout this study, we performed multi-site (MS) optimisations, i.e., optimizations executed over multiple sites of the same PFT simultaneously in order to find one common set of optimised parameters. Each optimization was run for 20 iterations, which we found to be sufficient for the system to converge. For each iteration, 32 chromosomes were used i.e., 32 different combinations of parameter values. We left the last year of each Fluxnet site out of the optimisation to have independent data for the validation step of the analysis.

200 The first set of optimizations tested two different combinations of gross and net carbon fluxes:



- **[Flx_{GR}]** 2 MS optimizations against daily GPP and TER, one for all the TeBS sites and one for all the TeNE sites.
- **[Flx_{GN}]** 2 MS optimizations against daily GPP and NEE, one for all the TeBS sites and one for all the TeNE sites.

Note that GPP and TER are derived from NEE with $NEE=TER-GPP$. This means that these data are model-derived estimates, which could introduce additional uncertainty to the results. However, by separating the fluxes we get a better understanding of the underlying mechanisms constraining two different ecosystem functions and are able better to diagnose the overestimations or underestimations of the assimilated processes, as initially discussed in Santaren et al. (2007). We are especially interested in the GPP constraint since this will give us an insight into plant productivity and will allow us to assess the CO₂ fertilising effect under nitrogen limitation. GPP is also directly used in the calculation of water use efficiency (WUE), here defined as the ratio between GPP and transpiration, one of the diagnostics we consider at the end of the study.

We further acknowledge that the data streams are not independent from each other. This poses a challenge when working in a Bayesian framework, especially when defining the **R** matrix in Eq. 1. Although there are methods for including the correlation between different data streams in the **R**, these are relatively new and require a lot of extra analysis beyond the scope of this study. Instead, we rely on the standard method of inflating variances (Chevallier, 2007).

The optimal parameters found by optimising against the Fluxnet sites improved the fit to contemporary data. However, it was unclear whether the predicative skill of the model was improved. Therefore, after assessing the Fluxnet results, the next step was to incorporate the FACE sites. Using a simultaneous approach, the FACE and Fluxnet sites were optimised together in this second set of experiments. This approach ensures that the information is not lost between steps, as could be the case in step-wise approach when the optimisations are done one after the other. The optimisation was set up to give a higher weight to the single FACE site in each case ($weight=n$ where n is the number of Fluxnet sites for the given PFT). Based on our results (see Sect. 3.1) and our motivation to better capture the productivity of the different ecosystems, we chose to focus on the former Fluxnet optimisation, i.e. the one against GPP and NEE. Each of the following FACE site experiments were performed simultaneously with a **[Flx_{GN}]** optimisation over the relevant PFT:

- **[Flx_{GN}-AMB]** 2 optimisations against annual NPP and daily LAI, one each for the DUKE and ORNL sites at ambient CO₂ concentrations, perform simultaneously with a GPP-NEE multisite Fluxnet optimisation.
- **[Flx_{GN}-ELE]** 2 optimisations against annual NPP and daily LAI, one each for the DUKE and ORNL sites at elevated CO₂ concentrations, perform simultaneously with a GPP-NEE multisite Fluxnet optimisation.
- **[Flx_{GN}-BOTH]** 2 optimisations against annual NPP and daily LAI, one each for the DUKE and ORNL sites with both ambient and elevated CO₂ concentrations simultaneously, perform simultaneously with a GPP-NEE multisite Fluxnet optimisation.

For the final part of this study, we considered the sensitivity of the simulated GPP, NPP, and WUE to CO₂ increase whilst keeping the other drivers constant. Each of the Fluxnet sites were tested by running idealised 100-year-long simulations starting from present-day atmospheric CO₂, 380 ppm, and increasing CO₂ by 1% per year, leading to a near tripling of CO₂ by the end



of the simulation. This was done for both the prior and optimised model, using default model parameters and [Fl_{XGN}-BOTH] model parameters, respectively.

235 3 Results

3.1 Fluxnet optimisations

The nitrogen cycle version of the ORCHIDEE model used in this study has not yet been optimised against Fluxnet data, although it has been extensively tuned manually. Therefore, the first step is to see whether the fluxes over the TeBS and TeNE sites are well represented in the model and whether they can be optimised using observed data. For the Fluxnet optimisation, two tests are conducted. The best-performing optimisation will serve as the starting point for the optimisations including data from the FACE sites. In this section, we present the results from both MS Fluxnet optimisations: Fl_{XGR} and Fl_{XGN}. Figure 1 shows the mean seasonal cycle across all Fluxnet sites for each PFT considered. We show the modelled GPP, TER and NEE fluxes against the observed time series.

For the deciduous sites (TeBS; Fig. 1 left-hand column), we see that both GPP and TER are overestimated by the prior model, and the NEE sink is underestimated. This overestimation is the most severe for TER, where the prior model simulates a maximum of approximately $9 \text{ gCm}^{-2}\text{d}^{-1}$ when the maximum TER observed is half that. In contrast, the overestimation for GPP is very slight found at and after the peak. Both optimisations improve the model-data fit against GPP by correcting the overestimation found after the peak. Fl_{XGN} performs the best, with the average seasonal peak now being the same as the observations. Fl_{XGR} on the other-hand reduces peak below that observed. Similarly, both optimisation now starts production later in the year degrading the fit to the observations in the early months. In ORCHIDEE, deciduous sites lose all their leaves in winter and therefore, no photosynthesis occurs before the leaves start growing back in spring. In contrast, the observations never go to zero, implying there is undergrowth or evergreen vegetation present that we are not accounting for in the model set-up. When looking at the RMSD of the individual sites, we also see that Fl_{XGN} reduces the spread relatively to the prior. For TER, both optimisations improve the model-data fit over the whole period with Fl_{XGR} performing slightly better. This is not surprising since this optimisation directly considers the TER component of NEE. The optimisations mainly change the magnitude of the peak and do not correct for its late timing. When looking at the RMSD, we can see that a group of sites are driving the overestimation of TER with values close to 4.5 - this is corrected for in both optimisations. For NEE, the Fl_{XGN} optimisation performs better than Fl_{XGR}, especially in fitting the autumn month. However, because of the overestimation of summer TER with this parameter set means we do not attain the minimum of the NEE trough. We note that for NEE, the posterior spreads of RMSE over all sites are the same for both optimisations.

For the evergreen sites (TeNE; Fig. 1 right-hand column), the optimisations improve the GPP underestimation in the prior model by increasing the peak by approximately $2.5 \text{ gCm}^{-2}\text{d}^{-1}$. However, this falls short of correcting of the full overestimation, which is closer to $4 \text{ gCm}^{-2}\text{d}^{-1}$. The Fl_{XGN} optimisation performs best with the timing of the average peak closest to the observed value. However, both optimisations degrade the average fit to TER, increasing the overestimation found when using the prior set of parameters. Both optimisations move the summer peak up by between $0.5\text{-}1 \text{ gCm}^{-2}\text{d}^{-1}$, with Fl_{XGN} increasing

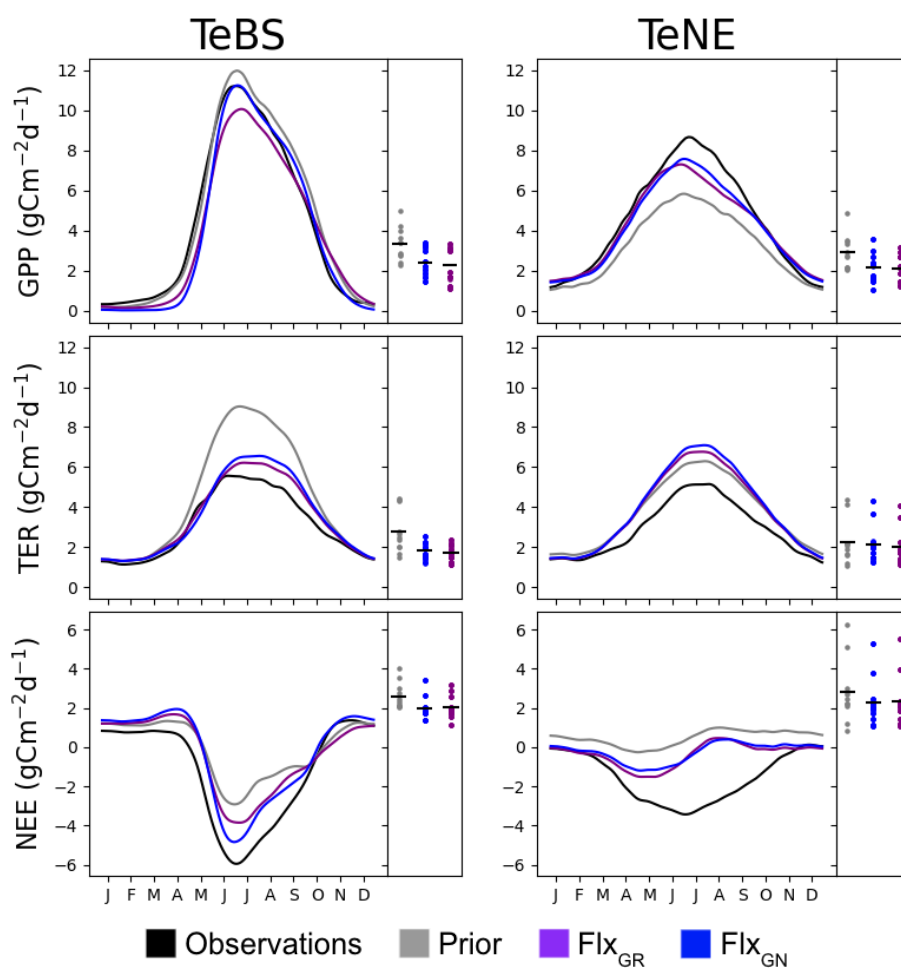


Figure 1. The main panel in each column shows the PFT-averaged mean seasonal cycles of daily observed and simulated GPP, TER, and NEE fluxes using different parameter values. The side panels show the model-data RMSD for the daily time series at each site, with the black horizontal bars showing the mean value across the sites.



the most. When considering the fit of the individual sites (right-hand part of each panel), we note that two anomalous sites are driving this behaviour. These sites (IT-Lav and US-Wi4) have respiration rates much lower than the other sites. Since we cannot match the respiration rates, we cannot capture the full NEE dip in summer. However, the improved GPP with both optimisations does mean that the NEE is slight improved compared to the prior mode.

270 In these optimisations, we have included a parameter, KSoil, which acts as a multiplicative factor of the initial soil and nitrogen pools (slow, passive and labile). We have used such a parameter in past ORCHIDEE optimisations at Fluxnet sites (e.g., Kuppel et al., 2012; Peylin et al., 2016; Bastrikov et al., 2018; Bacour et al., 2022) and found it played a large role in improving the model-data fit against respiration. Therefore, it seems counter-intuitive that we do not improve the fit to respiration as much as expected when including KSoil in the ORCHIDEE v3 optimisations, especially for the TeNE sites.

275 The past ORCHIDEE experiments all used a previous version of ORCHIDEE without the nitrogen cycle, so this factor solely acted on the carbon pools and heterotrophic respiration. Here KSoil multiplies both carbon and nitrogen pools to maintain the carbon/nitrogen ratio. However, by acting on the nitrogen pools, we directly impact on the mineralization rate and thus indirectly on plant N uptake, leaf N content, Vmax and, therefore, GPP. Whereas KSoil used only to impact soil respiration, it now impacts both respiration and GPP, and so the optimisation needs to find a compromise to fit both. To adjust the respiration,

280 Ksoil is decreased, reducing the carbon and nitrogen pools in the soils, but, at the same time, GPP is significantly reduced, deteriorating its fit to observations.

Overall, the ORCHIDEE model reasonably represents the TeBS and TeNE carbon fluxes, although respiration in the TeNE sites is high, even after optimisation. The Flx_{GN} optimisation results in the best-simulated production for both types of vegetation.

285 3.2 Incorporating data from the FACE sites

Given the results from the previous section, and our motivation to improve the model performance regarding ecosystem productivity, we will further include the FACE data to the Flx_{GN} optimisation.

3.2.1 Improving simulated NPP values

At ORNL, we can see in Fig. 2 that the uncalibrated version of ORCHIDEE (prior) overestimates the yearly NPP both under ambient and elevated conditions. This is consistent with prior GPP overestimation observed at the TeBS Fluxnet sites (Fig. 1).

290 When using parameters from the Fluxnet only optimisation (Flx_{GN}), we partly reduce this overestimation. For both CO_2 conditions, including FACE data as an additional constraint to the optimisation (Flx_{GN-AMB} , Flx_{GN-ELE} and $Flx_{GN-BOTH}$) improves the estimation of NPP compared to solely relying on the data from the Fluxnet sites. Under all atmospheric CO_2 conditions, Flx_{GN-ELE} reduces the RMSD the most followed by $Flx_{GN-BOTH}$ and then by Flx_{GN-AMB} . We would expect the latter to perform best at fitting NPP_{AMB} since it uses the observations in the optimisation, unlike Flx_{GN-ELE} . However, as we

295 will see later in Fig. 3, this is because the fit to LAI, the other part of the cost function, is improved most with the Flx_{GN-AMB} optimisation.



When considering the NPP ratio (elevated over ambient values) at ORNL, we see that the observations show a decreasing trend suggesting a possible progressive nitrogen limitation. The prior model is unable to capture this trend with a fixed ratio of around 1.3. Similarly, the Fluxnet only and the optimisation under ambient conditions do not mimic this decreasing trend. When using the FACE data from the elevated experiments in optimisation (Fl_{XGN}-ELE and Fl_{XGN}-BOTH, the resulting ratio trend is negative. The observations of NPP_{AMB} and NPP_{ELE} clearly show a slight decrease of NPP for the last years of the observations. Based on additional experiments, it has been shown that this limitation is due to nitrogen limitation (Norby et al., 2010). Again the prior does not capture the NPP decrease. For optimisations, Fl_{XGN}-ELE and Fl_{XGN}-BOTH may show a small signal, although it's not so obvious. This leads us to think that ORCHIDEE does not reproduce the dynamic of nitrogen in the soil well, notably the reduction of nitrogen availability for the plant, at least for this site. It is also possible that the model starts with too large a nitrogen content in the soil. Since parameter optimisation is insufficient at capturing this trend, we would instead need structural changes to the ORCHIDEE land surface model or possibly set a better initial nitrogen available content.

For DUKE, the prior model underestimates the NPP values under both CO₂ conditions, which again is coherent with GPP fit seen at the other TeNE sites (Fig. 1). The optimisation against Fluxnet data corrects this underestimation slightly. However, it is only by including the FACE data to the optimisation that we get the right magnitude and start getting the right inter-annual pattern. In each case, the optimisation performing best is the one that includes the relevant observations, i.e., Fl_{XGN}-AMB under ambient conditions and Fl_{XGN}-ELE under elevated conditions. The Fl_{XGN}-BOTH optimisation is able to fit both the ambient and elevated data reducing the RMSD to a similar extent as the best optimisation. When considering the elevated over ambient NPP ratio for DUKE, we see that the prior model and the Fluxnet-only optimisation (Fl_{XGN}) are the worse with values below one. Values below one suggest the forest is less productive under increased atmospheric CO₂. When looking more closely at the ORCHIDEE simulations for these parameter settings, we found that the mean-annual GPP under elevated conditions is higher than GPP under ambient conditions. Therefore, changes autotrophic respiration are responsible for the negative NPP ratio at the site. Autotrophic respiration is a function of leaf nitrogen content. The more nitrogen, the more respiration. It is, therefore, possible that the autotrophic respiration sensitivity to leaf nitrogen is too high in the model for TeNE under these parameter settings, at least at the DUKE site. The optimisations using FACE data do much better at simulating positive ratios with Fl_{XGN}-BOTH performing best. However, none of the optimisations constantly achieve the high magnitude of around 1.3 in the observations.

3.2.2 Improving the fit of leaf-area index

During the FACE experiments, we also optimised the model against daily LAI values (Fig. 3) since this allows us to capture some of the sub-annual variability driving NPP. For ORNL, under ambient and elevated CO₂, the prior model overestimates the LAI, peaking late and keeping its leaves late into the winter. The optimisation against the Fluxnet sites partly fixes both of these issues, bringing forward the leaf fall and decreasing the seasonal peak to 65% of the observed peak. When adding the FACE data under ambient conditions to the optimisation (i.e., Fl_{XGN}-AMB) we get the best fit, although the peak is still underestimated. The optimisation against both atmospheric conditions (Fl_{XGN}-BOTH) performs similarly to Fl_{XGN}-AMB. When we only add the elevated data to the optimisations, we do the worst of the FACE optimisations, with the summer peak nearly half of the

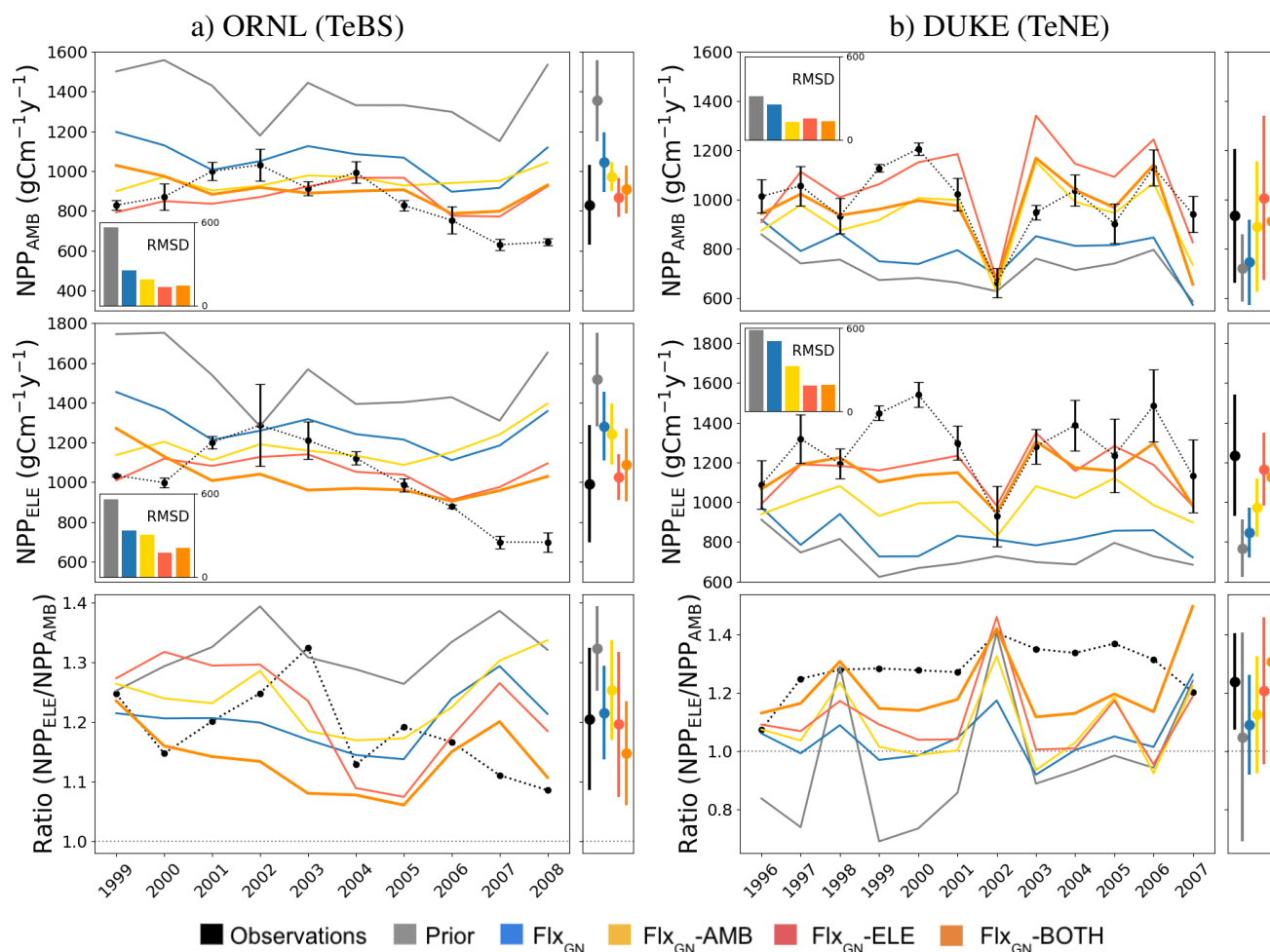


Figure 2. Time series of annual NPP under ambient (NPP_{AMB} ; top) and elevated (NPP_{ELE} ; middle) CO_2 conditions for each of the ORNL (a) and Duke (b) FACE sites. The ratios between NPP under elevated conditions and NPP under ambient conditions are shown in the bottom row, with a dotted-grey line indicating where the ratio is 1. The observations are shown in black, with error bars. The coloured lines represent different ORCHIDEE model simulations under different parameter sets - prior refers to the standard ORCHIDEE run using uncalibrated parameters, and the different “Flx” runs denote the data streams used in the optimisations (defined in Sect. 2.4). The bar chart insert in each time series panel shows the RMSD between the observations and each model run. The multi-annual NPP mean \pm its standard deviation is shown next to each panel.

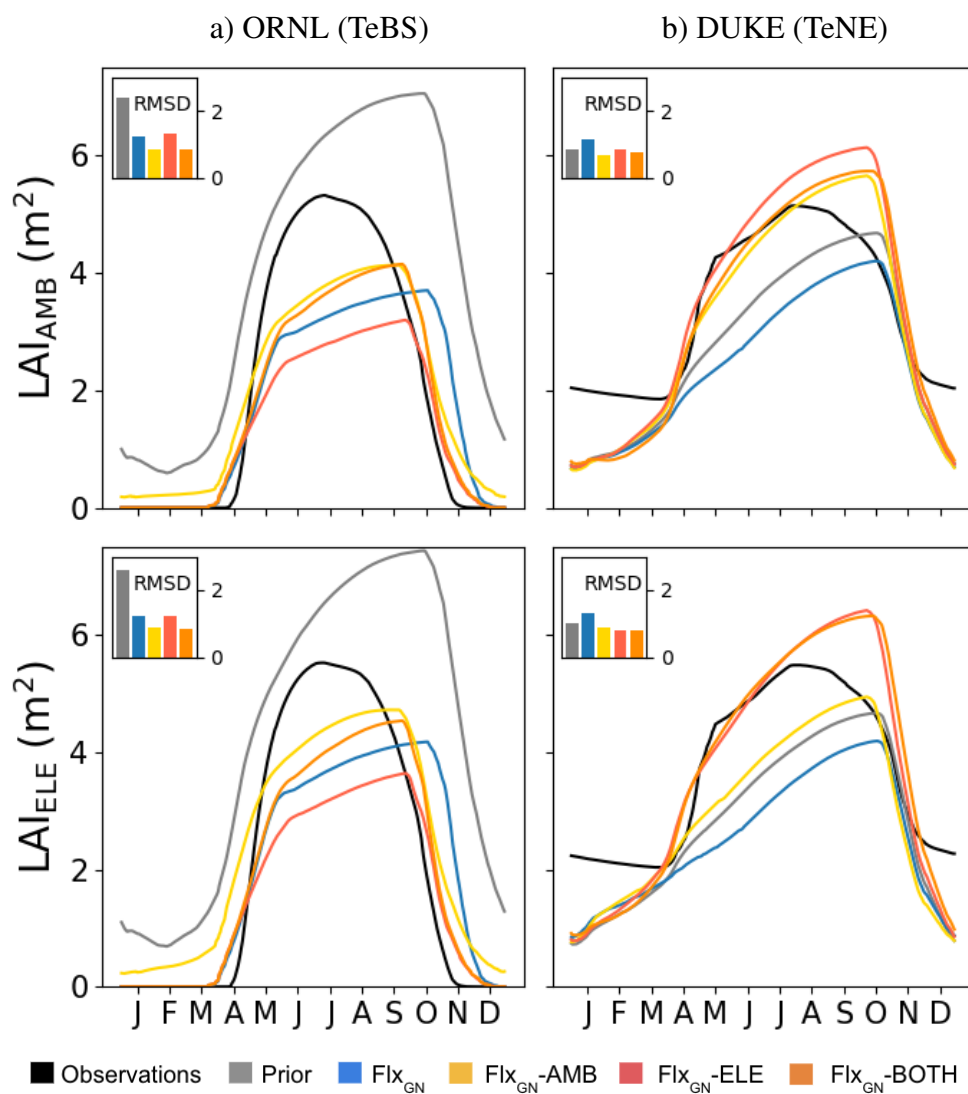


Figure 3. Model fit against seasonal LAI under different parameter sets at ORNL and DUKE. LAI under ambient CO₂ conditions (LAI_{AMB}) shown in the top row and elevated CO₂ conditions (LAI_{ELE}) on the bottom row. The bar chart inset in each panel shows the RMSD between the observations and the model.

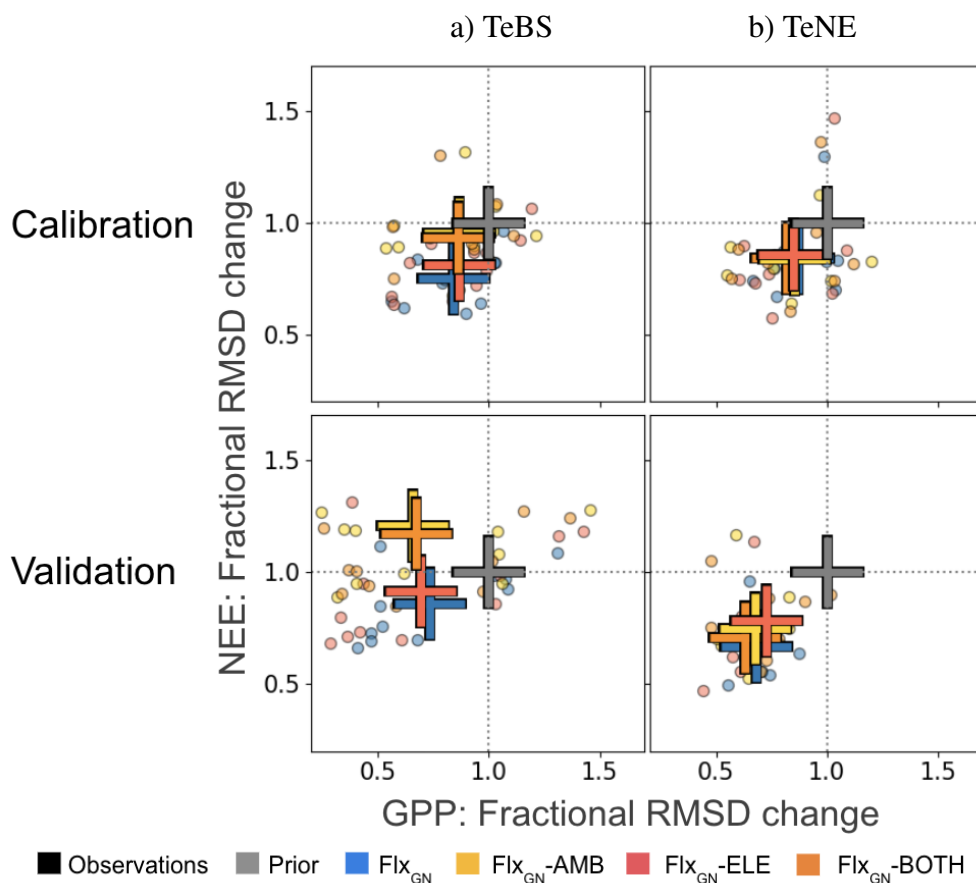


Figure 4. Fractional change in model-data RMSD for daily NEE and GPP at each site grouped by PFT obtained by the different optimisations. Fractional change is calculated by dividing the posterior RMSD by the prior RMSD (i.e., $\text{RMSD}[y, M(\mathbf{x}_{opt})]/\text{RMSD}[y, M(\mathbf{x}_b)]$ using the notation in Sect. 2.2). Values below 1 represent an improvement in model-data fit, whereas values above 1 represent an increase in RMSD compared to the prior run. The crosses show the mean value across the sites for a given optimal parameter set.

observed. This explains why $\text{Flx}_{\text{GN-ELE}}$ outperformed $\text{Flx}_{\text{GN-AMB}}$ in fitting NPP at ORNL (Fig. 2). By improving NPP to a large extent than $\text{Flx}_{\text{GN-AMB}}$, $\text{Flx}_{\text{GN-ELE}}$ was unable to improve the LAI as much. This highlights one of the common issues with multi-stream data assimilation - improving the fit against one data stream can be part of a trade-off against another.

335 Sometimes this can even be a degradation compared to the prior. Finally, although leaves are kept into the winter, unlike in the observations, the LAI seasonality is much improved in the optimisations compared to the prior model.

3.2.3 Maintaining the fit to the Fluxnet sites

The misfit part of the cost function (i.e., measuring the difference between the model and observations) is made up of two components during the FACE optimisations. The first is the fit of the FACE site to annual NPP (Fig. 2) and daily LAI (Fig. 3)



340 under ambient or evaluated conditions. The second is the fit of the multiple Fluxnet sites to daily GPP and NEE. Although the
FACE component was weighted during the optimisation (see section 2.4), it is important that we maintain a good model-data
fit for the Fluxnet sites to ensure confidence in the optimised parameter values. In Fig. 4, we consider the fractional change
in model-data RMSD (calculated by dividing the posterior RMSD by the prior RMSD). For both vegetation types, the best
improvement against both GPP and NEE is found when using parameters from the experiment solely optimising over the
345 Fluxnet sites (Flx_{GN}). This is true for both the optimisation years, i.e., the years used in the optimisation, and the validation
year, i.e., the year of independent data omitted from the optimisation. Adding further constraints by including FACE data
reduces the improvement in model-data fit. After all, even though they are closely related, the FACE optimisations looked at
improving the fit to NPP and LAI, not GPP and NEE. However, the sets of parameters obtained from these latter optimisations
will give a better compromise for both the FACE and Fluxnet sites.

350 For the TeBS sites, on average, we improve the fit to GPP over the optimisation years to the same extent for all optimisations.
Slightly higher reductions in fractional GPP RMSD change are observed for the validation year. However, for NEE, fractions in
RMSD are different depending on the optimisation - with the ambient and both optimisations resulting in the smallest decreases
for the calibration years. For the validation, these two optimisations degraded the fit for the validation year (20%).

In contrast, for the TeNE sites against the calibration years, the optimisations all give similar reductions in the model-data
355 fit RMSD for both NEE and GPP. When confronted with the validation year, the response is more spread out, with the Fluxnet
only optimisation performing the best, closely followed by Flx_{GN} -BOTH.

For the validation, we only used one year of data, which helps to explain why the results are more spread out. With one year
of data, we are more susceptible to specifics of that given year instead of to trends over a longer period. Ideally, we would want
to validate over a larger period. However, some of the sites in this study only had a few years in their data record, making this
360 not possible.

3.3 Projections using the optimised models

To conclude this study, we test how the optimised model parameters impact the model responses to CO_2 increase. We espe-
cially want to consider the additional information gained from including FACE data in the optimisation. As such, for this last
experiment, we use parameters of the Flx_{GN} (Fluxnet only) and Flx_{GN} -BOTH (Fluxnet and FACE data) optimisations. The
365 Flx_{GN} -BOTH optimisation resulted in the best compromise in simulating NPP at ambient and elevated conditions, as well as
their ratio, while also maintaining a satisfying model-data fit to GPP over the Fluxnet sites.

To test the model response to CO_2 increase, we run an idealised 100-year-long experiment increasing CO_2 1% per year over
all the Fluxnet sites. This is similar to the experiment done in Vuichard et al. (2019) where the model was also assessed with
GPP, transpiration and WUE. Note that the prior projections shown here are similar to those obtained in Vuichard et al. (2019).
370 We first note that the optimised models predict higher starting values of GPP, Transpiration and WUE for TeBS when compared
to the prior model (Table 3). This is consistent with Fig. 1 and 2, where for TeBS, the prior had the highest productivity. Similar,
the behaviour for TeNE sites mirrors earlier findings - the prior model underestimated productivity. The optimisations lead to
higher starting values (except for WUE), and including data from FACE is found to induce a larger increase.

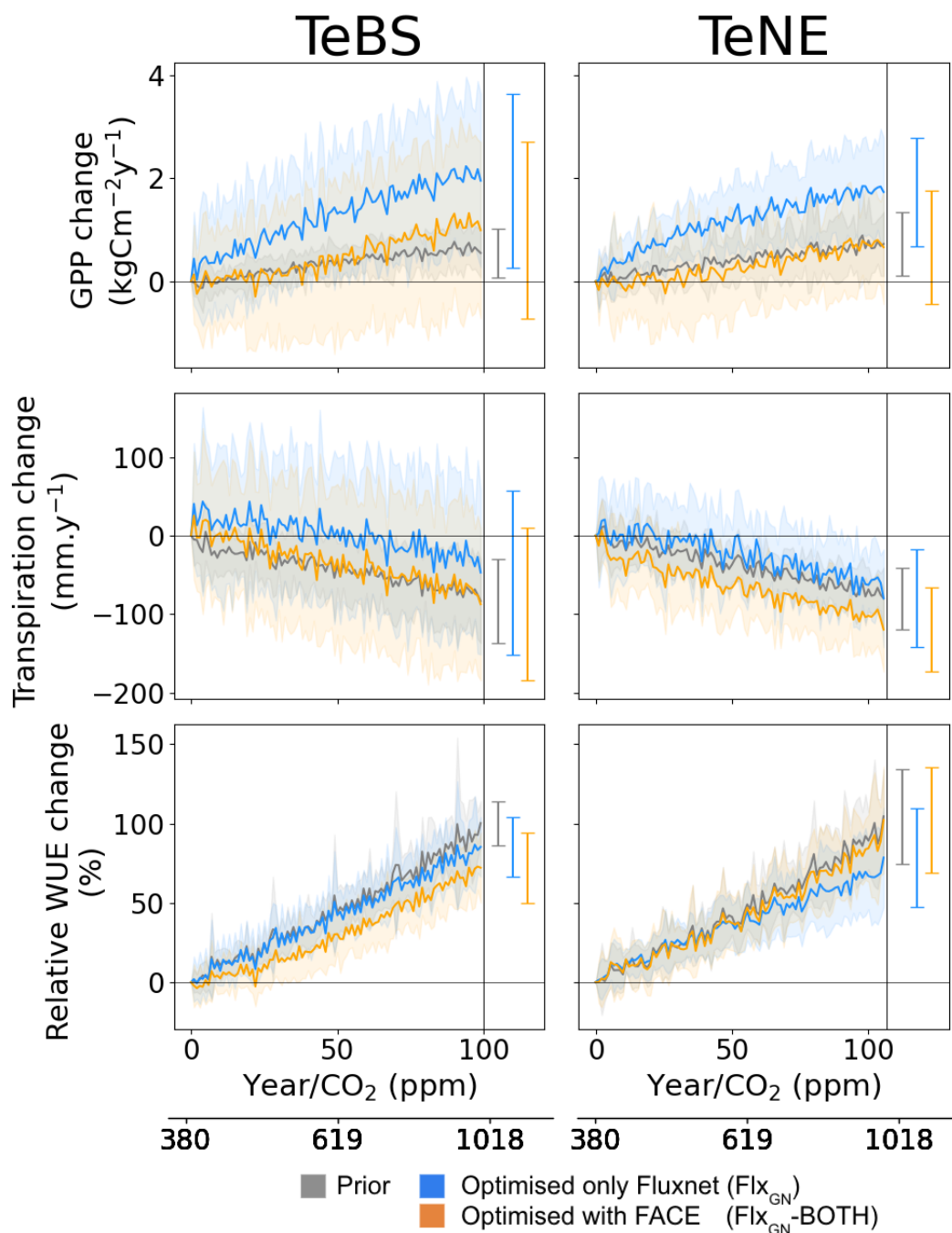


Figure 5. Effect of changes in the atmospheric CO₂ concentration on GPP, NPP and Water Use Efficiency (WUE) for different model parameter sets. Atmospheric changes are represented by 1%CO₂ increase per year. The prior model (grey) and optimised model (Flx_{GN}-BOTH; orange) were run at each Fluxnet site (see Table. 2). The thick lines represent the mean simulated across all sites, while the shaded areas represent the standard deviation. The mean and standard deviation at the end of the 100-year simulation are shown in the right-hand side of each panel.



	TeBS			TeNE		
	Prior	Optimised		Prior	Optimised	
		Fluxnet only	Fluxnet and FACE		Fluxnet only	Fluxnet and FACE
GPP ($\text{kgCm}^{-2}\text{y}^{-1}$)	5.22 + 0.55	3.58 + 1.95	4.03 + 0.99	2.85 + 0.73	3.93 + 1.73	4.59 + 0.66
Transpiration (mm.y^{-1})	417.29 - 83.43	342.93 - 47.06	365.57 - 87.52	242.62 - 80.05	313.35 - 79.92	357.47 - 119.82
WUE (%)	123.46 + 100.21	104.64 + 85.25	110.13 - 72.14	114.76 + 104.48	95.17 + 78.5	127.85 + 102.21

Table 3. Mean values at the start of the 100-year experiment and net change by the end of the experiment for the prior model and the optimised models.

In Fig. 5, we consider the net increase over the 100-year simulation. For both vegetation types, the rate of increase of GPP found by using parameters from the Fluxnet-only optimisation is the highest. For TeNE, the curve is starting to plateau due to a progressive nitrogen limitation. However, in both cases, the rate of increase is much faster compared to the runs with parameters from the Flx_{GN} -BOTH optimisation. The fertilisation rate decreases compared to the Fluxnet only optimisation. In Fig. 2, we saw that the Flx_{GN} -BOTH optimisation was starting to model the declining productivity response at ORNL. We may still be overestimating the fertilisation effect over TeBS sites and we could expect an even stronger response to nitrogen limitation - further reducing this GPP increase. Although the GPP increase is similar to the prior model for forest types, the larger spread among sites for Flx_{GN} -BOTH is notable - with negative GPP change at some sites suggesting a stronger nitrogen limitation under these parameters.

For transpiration rates over both TeBS and TeNE, the Flx_{GN} simulations result in the smallest change by the end of the century. In contrast, the simulations Flx_{GN} -BOTH result in the largest change. For WUE, the differences observed in GPP and transpiration are mostly cancelled out and therefore, the different parameters do not illicit a great variation in responses. For TeBS, the prior and Flx_{GN} simulations give a similar increase, with Flx_{GN} -BOTH suggests a slightly weaker increase. For TeNE, it is the opposite - Flx_{GN} is slightly weaker than the other two simulations.

Note that our experiment only looks at increasing CO_2 while keeping the other drivers constant. It is possible that we would see different responses if we were to include changes in meteorological forcing (to mimic climate change) or changes in nitrogen deposition and fertilisation, which would change nitrogen limitation and responses to water stress. Although we performed a sensitivity analysis to select the parameters, it is possible that additional parameters (e.g., ones controlling water stress or controlling the allocation of carbon in the plant) will give a different response. Furthermore, direct structural changes or addition to the model code could also change the results. Nevertheless, the fact that different parameters give such a varied model response to elevated CO_2 for a given model structure highlights the importance of finding a robust set of parameters to have faith in. When performing the Fluxnet optimisations, the optimisation against GPP and NEE gave the best fit to both quantities resulting in sets of parameters that worked well across each PFT. However, when considering production through NPP and LAI under different atmospheric CO_2 conditions, we found that the parameters were unable to capture the differences observed in data under different CO_2 regimes. Instead, the parameter sets found by optimising the model against Fluxnet data and both ambient and elevated CO_2 conditions were found to be more robust. These parameters resulted in the best fits overall



400 against NPP and LAI under two different CO₂ regimes. As such, we have more confidence in these parameters and their ability to simulate terrestrial production under different atmospheric CO₂ conditions, leading us to have more faith in the model projections performed with them.

4 Conclusions

As our terrestrial models become more complex through the addition of more processes, we need to confront them with
405 observed data to ensure we have confidence in the model's predictions. Manipulation experiments allow us to test the model under different CO₂ regimes and its capabilities to reproduce the ecosystem responses. By optimising model parameters against data from both ambient and elevated atmospheric CO₂ conditions, we gain confidence in the model's ability to reproduce fluxes under different atmospheric conditions. We find the production is currently underestimated in the model, and the strength of the CO₂ fertilization effect changes depending on the type of forest considered. It will be interesting to use these parameters
410 further to assess the evaluation of carbon stocks under high concentrations of CO₂ and at a larger scale to evaluate more directly the impact on the global sink.

We find that through the different optimisations of this carbon-nitrogen version of ORCHIDEE, we are able to improve the representation of simulated productivity. All optimisations are able to improve modelled GPP, and we generally improve the magnitude for NPP for the two levels of atmospheric CO₂. However, we do not achieve as good an improvement against
415 respiration and, therefore, against NEE. Although we are unable to capture fully the inter-annual variability of NPP after optimisation, at ORNL we do start to model a negative trend for the NPP ratio, which is apparent in the observations but not simulated in the prior model. This suggests that the optimised parameters are able to capture the progressive nitrogen limitation at this site. We do struggle to capture the seasonal cycle of LAI properly at both FACE sites, suggesting incorrect LAI allocation. These results highlight the fact that optimising an LSM with the nitrogen cycle is more difficult and complex than with a carbon-
420 only LSM, given the increased model feedbacks. Overall the current optimisation performs slightly worse than compared to the prior optimisations of previous ORCHIDEE versions (e.g., Kuppel et al., 2012). One example of increased model feedbacks is through the KSoil parameter. Without the nitrogen cycle, by changing the initial carbon stocks, this parameter was able to fix the magnitude of the respiration flux. However, the parameter now also changes the initial nitrogen stock and hence the mineralisation flux in the soil, which impacts GPP.

425 Although the optimisation is not as optimal as that achieved with a carbon-only model, this work opens a new avenue to validate LSMs quantitatively with FACE data. We see that not only is there a benefit of adding FACE data on top of Fluxnet data when optimising a land surface model, it is, in fact, risky not to. The Fluxnet-only optimisations do not perform well under elevated conditions, which is critical when predicting the terrestrial response to climate change. Furthermore, since we see that the future evolution of terrestrial productivity change is sensitive to the parameter values used in the model, getting these
430 parameters right is critical. This is notable for both vegetation types where the Fluxnet-only optimisations and the optimisations with FACE data give very different trajectories in the idealized 1% CO₂ experiments, with the Fluxnet-only optimisations likely overestimating the CO₂ fertilisation effect.



By optimising the model against a number of different constraints, we can reduce parameter uncertainty and hence reduce uncertainty in the projections. Such experiments can help us to describe better the future fertilizing effect of CO₂ under possible nitrogen limitation. However, we find that in our study, two sites are not sufficient to draw such conclusions about terrestrial responses to elevated CO₂, which could vary over different ecosystems. Although we have shown this approach of joint optimisations to be promising, more sites are needed. It would also be interesting to have different levels of nitrogen input at these sites to assess more clearly the nitrogen limitation on the CO₂ fertilization effect. We are also limited by the data the sites can provide. Due to the CO₂ fumigation over FACE sites, daily NEE cannot be measured at FACE sites, and therefore, GPP and TER estimates cannot be derived. These variables are more directly linked to productivity than leaf area index, the variable we use in our optimisations. There are other processes at play that also need to be assessed. For example, the effect of soil moisture and the stress response to water availability will also impact the mineralisation of organic matter and, thus, nutrient availability. Finally, structural changes do need to be made to the model to better capture the inter-annual variability of simulated NPP and LAI.

Nevertheless, although it is by no means exhaustive, this proof-of-concept experiment highlights the importance of manipulation experiments and the additional information they can provide for model improvement. This is the first study of a global process-based model using data in this way. With more FACE sites, these types of data could be used more consistently as part of the model optimisation procedures. Other data streams, such as normalized difference vegetation index, solar-induced fluorescence satellite data, and tree rings, could also be used to complement such optimisations giving the best constraints on the model parameters and hence on future climate predictions.

Code availability. The source code for the ORCHIDEE version used in this model is freely available online via the following address: <https://doi.org/10.14768/c429d5c4-1164-45a7-8556-9bbef31baee3>, and the optimisation tool is available through a dedicated web site for data assimilation with ORCHIDEE (<https://orchidas.lsce.ipsl.fr>).

Author contributions. PP and NR conceived of the experiment. LE performed the preliminary experiments. NV developed the nitrogen version of the ORCHIDEE. VB developed the data assimilation system, which NR adapted to FACE experiments. BG provided the FACE data and configuration files needed for ORCHIDEE. AL provided expertise first running ORCHIDEE-CN. NR ran the main experiments and generated the figures. All authors contributed to writing and editing the manuscript.

Competing interests. The author declare no competing interesting

Acknowledgements. This work used eddy covariance data acquired and shared by the FLUXNET community, including these networks: AmeriFlux, AfriFlux, AsiaFlux, CarboAfrica, CarboEuropeIP, CarboItaly, CarboMont, ChinaFlux, Fluxnet-Canada, GreenGrass, ICOS,



KoFlux, LBA, NECC, OzFlux-TERN, TCOS-Siberia, and USCCC. The FLUXNET eddy covariance data processing and harmonization was carried out by the ICOS Ecosystem Thematic Center, AmeriFlux Management Project and Fluxdata project of FLUXNET, with the support of CDIAC, and the OzFlux, ChinaFlux and AsiaFlux offices. This work also data from the FACE experiments: Oak Ridge National Laboratory and DUKE Forest.

465 We would also like to thank the wider ORCHIDEE development team for developing and maintaining the ORCHIDEE land surface model. We acknowledge the support by the ESM2025 project. This project has received funding from the European Union's Horizon 2020 research and innovation programme under grant agreement No 101003536. We also acknowledge funding from the European Union's Horizon 2020 research and innovation programme under the Marie Skłodowska-Curie grant agreement No 101020076.



References

- 470 Ainsworth, E. A. and Long, S. P.: What have we learned from 15 years of free-air CO₂ enrichment (FACE)? A meta-analytic review of the responses of photosynthesis, canopy properties and plant production to rising CO₂, *New phytologist*, 165, 351–372, 2005.
- Ainsworth, E. A. and Long, S. P.: 30 years of free-air carbon dioxide enrichment (FACE): What have we learned about future crop productivity and its potential for adaptation?, *Global Change Biology*, 27, 27–49, 2021.
- Bacour, C., MacBean, N., Chevallier, F., Léonard, S., Koffi, E. N., and Peylin, P.: Assimilation of multiple different datasets results in large
475 differences in regional to global-scale NEE and GPP budgets simulated by a terrestrial biosphere model, *Biogeosciences Discussions*, pp. 1–42, 2022.
- Bastrikov, V., Macbean, N., Bacour, C., Santaren, D., Kuppel, S., and Peylin, P.: Land surface model parameter optimisation using in situ flux data: Comparison of gradient-based versus random search algorithms (a case study using ORCHIDEE v1.9.5.2), *Geoscientific Model Development*, 11, 4739–4754, <https://doi.org/10.5194/gmd-11-4739-2018>, 2018.
- 480 Bonan, G.: *Ecological climatology: concepts and applications*, Cambridge University Press, 2015.
- Boucher, O., Servonnat, J., Albright, A. L., Aumont, O., Balkanski, Y., Bastrikov, V., Bekki, S., Bonnet, R., Bony, S., Bopp, L., et al.: Presentation and evaluation of the IPSL-CM6A-LR climate model, *Journal of Advances in Modeling Earth Systems*, 12, e2019MS002 010, 2020.
- Byrd, R. H., Lu, P., Nocedal, J., and Zhu, C.: A limited memory algorithm for bound constrained optimization, *SIAM Journal on scientific
485 computing*, 16, 1190–1208, 1995.
- Caldararu, S., Thum, T., Yu, L., and Zaehle, S.: Whole-plant optimality predicts changes in leaf nitrogen under variable CO₂ and nutrient availability, *New Phytologist*, 225, 2331–2346, 2020.
- Chaney, N. W., Herman, J. D., Ek, M. B., and Wood, E. F.: Deriving global parameter estimates for the Noah land surface model using FLUXNET and machine learning, *Journal of Geophysical Research: Atmospheres*, 121, 13–218, 2016.
- 490 Chevallier, F.: Impact of correlated observation errors on inverted CO₂ surface fluxes from OCO measurements, *Geophysical Research Letters*, 34, 2007.
- De Kauwe, M. G., Medlyn, B. E., Zaehle, S., Walker, A. P., Dietze, M. C., Hickler, T., Jain, A. K., Luo, Y., Parton, W. J., Prentice, I. C., et al.: Forest water use and water use efficiency at elevated CO₂: A model-data intercomparison at two contrasting temperate forest FACE sites, *Global change biology*, 19, 1759–1779, 2013.
- 495 De Kauwe, M. G., Medlyn, B. E., Zaehle, S., Walker, A. P., Dietze, M. C., Wang, Y.-P., Luo, Y., Jain, A. K., El-Masri, B., Hickler, T., et al.: Where does the carbon go? A model–data intercomparison of vegetation carbon allocation and turnover processes at two temperate forest free-air CO₂ enrichment sites, *New Phytologist*, 203, 883–899, 2014.
- De Kauwe, M. G., Medlyn, B. E., Walker, A. P., Zaehle, S., Asao, S., Guenet, B., Harper, A. B., Hickler, T., Jain, A. K., Luo, Y., et al.: Challenging terrestrial biosphere models with data from the long-term multifactor Prairie Heating and CO₂ Enrichment experiment,
500 *Global Change Biology*, 23, 3623–3645, 2017.
- de Rosnay, P. and Polcher, J.: Modelling root water uptake in a complex land surface scheme coupled to a GCM, <https://doi.org/10.5194/hess-2-239-1998>, 1998.
- Ducoudré, N. I., Laval, K., and Perrier, A.: SECHIBA, a new set of parameterizations of the hydrologic exchanges at the land-atmosphere interface within the LMD atmospheric general circulation model, *Journal of Climate*, pp. 248–273, 1993.



- 505 Fisher, R. A., Wieder, W. R., Sanderson, B. M., Koven, C. D., Oleson, K. W., Xu, C., Fisher, J. B., Shi, M., Walker, A. P., and Lawrence, D. M.: Parametric Controls on Vegetation Responses to Biogeochemical Forcing in the CLM5, *Journal of Advances in Modeling Earth Systems*, 11, 2879–2895, <https://doi.org/10.1029/2019MS001609>, 2019.
- Friedlingstein, P., O’sullivan, M., Jones, M. W., Andrew, R. M., Hauck, J., Olsen, A., Peters, G. P., Peters, W., Pongratz, J., Sitch, S., et al.: Global carbon budget 2020, *Earth System Science Data*, 12, 3269–3340, 2020.
- 510 Friedlingstein, P., O’sullivan, M., Jones, M. W., Andrew, R. M., Gregor, L., Hauck, J., Le Quéré, C., Luijkx, I. T., Olsen, A., Peters, G. P., et al.: Global carbon budget 2022, *Earth System Science Data*, 14, 4811–4900, 2022.
- Goldberg, D. E. and Holland, J. H.: *Genetic algorithms and machine learning*, 1988.
- Haupt, R. L. and Haupt, S. E.: *Practical genetic algorithms*, John Wiley & Sons, 2004.
- Knorr, W. and Kattge, J.: Inversion of terrestrial ecosystem model parameter values against eddy covariance measurements by Monte Carlo
515 sampling, *Global change biology*, 11, 1333–1351, 2005.
- Krinner, G., Viovy, N., de Noblet-Ducoudré, N., Ogée, J., Polcher, J., Friedlingstein, P., Ciais, P., Sitch, S., and Prentice, I. C.: A dynamic global vegetation model for studies of the coupled atmosphere-biosphere system, *Global Biogeochemical Cycles*, 19, 1–33, <https://doi.org/10.1029/2003GB002199>, 2005.
- Kuppel, S., Peylin, P., Chevallier, F., Bacour, C., Maignan, F., and Richardson, A.: Constraining a global ecosystem model with multi-site
520 eddy-covariance data, *Biogeosciences*, 9, 3757–3776, 2012.
- Lasslop, G., Reichstein, M., Papale, D., Richardson, A. D., Arneeth, A., Barr, A., Stoy, P., and Wohlfahrt, G.: Separation of net ecosystem exchange into assimilation and respiration using a light response curve approach: critical issues and global evaluation, *Global change biology*, 16, 187–208, 2010.
- Lurton, T., Balkanski, Y., Bastrikov, V., Bekki, S., Bopp, L., Braconnot, P., Brockmann, P., Cadule, P., Contoux, C., Cozic, A., et al.:
525 Implementation of the CMIP6 Forcing Data in the IPSL-CM6A-LR Model, *Journal of Advances in Modeling Earth Systems*, 12, e2019MS001940, 2020.
- Malenovsky, Z., Rott, H., Cihlar, J., Schaepman, M. E., García-Santos, G., Fernandes, R., and Berger, M.: Sentinels for science: Potential of Sentinel-1,-2, and-3 missions for scientific observations of ocean, cryosphere, and land, *Remote Sensing of environment*, 120, 91–101, 2012.
- 530 McCarthy, H. R., Oren, R., Johnsen, K. H., Gallet-Budynek, A., Pritchard, S. G., Cook, C. W., Ladeau, S. L., Jackson, R. B., and Finzi, A. C.: Re-assessment of plant carbon dynamics at the Duke free-air CO₂ enrichment site: Interactions of atmospheric [CO₂] with nitrogen and water availability over stand development, *New Phytologist*, 185, 514–528, <https://doi.org/10.1111/j.1469-8137.2009.03078.x>, 2010.
- Medlyn, B. E., Zaehle, S., De Kauwe, M. G., Walker, A. P., Dietze, M. C., Hanson, P. J., Hickler, T., Jain, A. K., Luo, Y., Parton, W., et al.: Using ecosystem experiments to improve vegetation models, *Nature Climate Change*, 5, 528–534, 2015.
- 535 Morris, M. D.: Factorial sampling plans for preliminary computational experiments, *Technometrics*, 33, 161–174, 1991.
- Naudts, K., Ryder, J., McGrath, M., Otto, J., Chen, Y., Valade, A., Bellasen, V., Berhongaray, G., Bönisch, G., Campioli, M., et al.: A vertically discretised canopy description for ORCHIDEE (SVN r2290) and the modifications to the energy, water and carbon fluxes, *Geoscientific Model Development*, 8, 2035–2065, 2015.
- Norby, R. J., Warren, J. M., Iversen, C. M., Medlyn, B. E., and McMurtrie, R. E.: CO₂ enhancement of forest produc-
540 tivity constrained by limited nitrogen availability, *Proceedings of the National Academy of Sciences*, 107, 19368–19373, <https://doi.org/10.1073/pnas.1006463107>, 2010.



- Pastorello, G., Trotta, C., Canfora, E., Chu, H., Christianson, D., Cheah, Y.-W., Poindexter, C., Chen, J., Elbashandy, A., Humphrey, M., et al.: The FLUXNET2015 dataset and the ONEFlux processing pipeline for eddy covariance data, *Scientific data*, 7, 1–27, 2020.
- Peylin, P., Bacour, C., MacBean, N., Leonard, S., Rayner, P., Kuppel, S., Koffi, E., Kane, A., Maignan, F., Chevallier, F., Ciais, P., and Prunet, P.: A new stepwise carbon cycle data assimilation system using multiple data streams to constrain the simulated land surface carbon cycle, *Geoscientific Model Development*, 9, 3321–3346, <https://doi.org/10.5194/gmd-9-3321-2016>, 2016.
- Post, H., Vrugt, J. A., Fox, A., Vereecken, H., and Hendricks Franssen, H.-J.: Estimation of Community Land Model parameters for an improved assessment of net carbon fluxes at European sites, *Journal of Geophysical Research: Biogeosciences*, 122, 661–689, 2017.
- Prentice, I. C.: Terrestrial nitrogen cycle simulation with a dynamic global vegetation model, *Global Change Biology*, 14, 1745–1764, 2008.
- 545 Raoult, N. M., Jupp, T. E., Cox, P. M., and Luke, C. M.: Land-surface parameter optimisation using data assimilation techniques: the adJULES system V1.0, *Geoscientific Model Development*, 9, 2833–2852, 2016.
- Santaren, D., Peylin, P., Viovy, N., and Ciais, P.: Optimizing a process-based ecosystem model with eddy-covariance flux measurements: A pine forest in southern France, *Global Biogeochemical Cycles*, 21, 2007.
- Santaren, D., Peylin, P., Bacour, C., Ciais, P., and Longdoz, B.: Ecosystem model optimization using in situ flux observations: Benefit of Monte Carlo versus variational schemes and analyses of the year-to-year model performances, *Biogeosciences*, 11, 7137–7158, <https://doi.org/10.5194/bg-11-7137-2014>, 2014.
- 555 Sulman, B. N., Shevliakova, E., Brzostek, E. R., Kivlin, S. N., Malyshev, S., Menge, D. N., and Zhang, X.: Diverse mycorrhizal associations enhance terrestrial C storage in a global model, *Global Biogeochemical Cycles*, 33, 501–523, 2019.
- Tarantola, A.: *Inverse problem theory and methods for model parameter estimation*, SIAM, 2005.
- 560 Vuichard, N. and Papale, D.: Filling the gaps in meteorological continuous data measured at FLUXNET sites with ERA-Interim reanalysis, *Earth System Science Data*, 7, 157–171, 2015.
- Vuichard, N., Messina, P., Luyssaert, S., Guenet, B., Zaehle, S., Ghattas, J., Bastrikov, V., and Peylin, P.: Accounting for carbon and nitrogen interactions in the global terrestrial ecosystem model ORCHIDEE (trunk version, rev 4999): multi-scale evaluation of gross primary production, *Geoscientific Model Development*, 12, 4751–4779, <https://doi.org/10.5194/gmd-12-4751-2019>, 2019.
- 565 Walker, A. P., Hanson, P. J., De Kauwe, M. G., Medlyn, B. E., Zaehle, S., Asao, S., Dietze, M., Hickler, T., Huntingford, C., Iversen, C. M., et al.: Comprehensive ecosystem model-data synthesis using multiple data sets at two temperate forest free-air CO₂ enrichment experiments: Model performance at ambient CO₂ concentration, *Journal of Geophysical Research: Biogeosciences*, 119, 937–964, 2014.
- Walker, A. P., De Kauwe, M. G., Fenstermaker, L. F., Hungate, B., Medlyn, B., Megonigal, P. J., Oren, R., Pendall, E., Talhelm, A. F., Zaehle, S., et al.: FACE-MDS Phase 2: Data from Six US-Located Elevated CO₂ Experiments, Tech. rep., Environmental System Science Data
- 570 Infrastructure for a Virtual Ecosystem . . . , 2018.
- Walker, A. P., De Kauwe, M. G., Medlyn, B. E., Zaehle, S., Iversen, C. M., Asao, S., Guenet, B., Harper, A., Hickler, T., Hungate, B. A., et al.: Decadal biomass increment in early secondary succession woody ecosystems is increased by CO₂ enrichment, *Nature Communications*, 10, 454, 2019.
- Walker, A. P., De Kauwe, M. G., Bastos, A., Belmecheri, S., Georgiou, K., Keeling, R. F., McMahon, S. M., Medlyn, B. E., Moore, D. J., Norby, R. J., et al.: Integrating the evidence for a terrestrial carbon sink caused by increasing atmospheric CO₂, *New Phytologist*, 229, 2413–2445, 2021.
- 575 Wieder, W. R., Lawrence, D. M., Fisher, R. A., Bonan, G. B., Cheng, S. J., Goodale, C. L., Grandy, A. S., Koven, C. D., Lombardozzi, D. L., Oleson, K. W., et al.: Beyond static benchmarking: Using experimental manipulations to evaluate land model assumptions, *Global Biogeochemical Cycles*, 33, 1289–1309, 2019.



- 580 Zaehle, S. and Dalmonech, D.: Carbon–nitrogen interactions on land at global scales: current understanding in modelling climate biosphere feedbacks, *Current Opinion in Environmental Sustainability*, 3, 311–320, 2011.
- Zaehle, S. and Friend, A. D.: Carbon and nitrogen cycle dynamics in the O-CN land surface model: 1. Model description, site-scale evaluation, and sensitivity to parameter estimates, *Global Biogeochemical Cycles*, 24, <https://doi.org/10.1029/2009GB003521>, 2010.
- Zaehle, S., Sitch, S., Smith, B., and Hatterman, F.: Effects of parameter uncertainties on the modeling of terrestrial biosphere dynamics, *Global Biogeochemical Cycles*, 19, 1–16, <https://doi.org/10.1029/2004GB002395>, 2005.
- 585 Zaehle, S., Medlyn, B. E., De Kauwe, M. G., Walker, A. P., Dietze, M. C., Hickler, T., Luo, Y., Wang, Y.-P., El-Masri, B., Thornton, P., et al.: Evaluation of 11 terrestrial carbon–nitrogen cycle models against observations from two temperate Free-Air CO₂ Enrichment studies, *New Phytologist*, 202, 803–822, 2014.